UCRL-JC-122393
PREPRINT
CONF-960672--2

"A Generalized Wavelet Extrema Representation"

Jian Lu, Martin Lades
Institute for Scientific Computing Research
Lawrence Livermore National Laboratory
Livermore, CA

This paper was prepared for submission to
IEEE Computer Society Conference on
Computer Vision Pattern Recognition '96
San Francisco, CA June 16 - 20, 1996

October, 1995

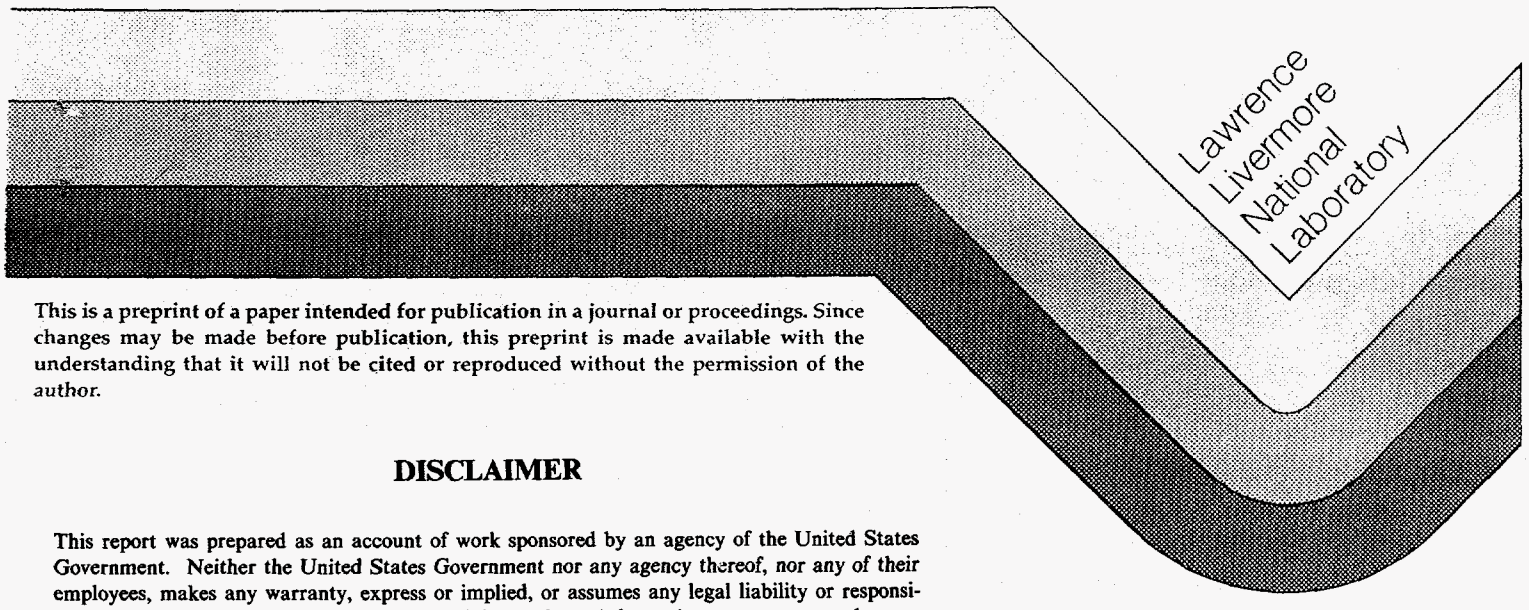

DISCLAIMER

A Generalized Wavelet Extrema Representation

Jian Lu and H. Martin Lades

Institute for Scientific Computing Research
Lawrence Livermore National Laboratory
P.O. Box 808, L-416
Livermore, CA 94551, U.S.A.

Email: jian@redhook.llnl.gov

October 20, 1995

Abstract: The wavelet extrema representation originated by Stéphane Mallat is a unique framework for low-level and intermediate-level (feature) processing. In this paper, we present a new form of wavelet extrema representation generalizing Mallat's original work. The generalized wavelet extrema representation is a feature-based multiscale representation. For a particular choice of wavelet, our scheme can be interpreted as representing a signal or image by its edges, and peaks and valleys at multiple scales. Such a representation is shown to be stable—the original signal or image can be reconstructed with very good quality. It is further shown that a signal or image can be modeled as piecewise monotonic, with all turning points between monotonic segments given by the wavelet extrema. A new projection operator is introduced to enforce piecewise monotonicity of a signal in its reconstruction. This leads to an enhancement to previously developed algorithms in preventing artifacts in reconstructed signal.

Categories: No good match to listed ones.
Keywords: Features, image representation, multiscale edges, wavelets.

A Generalized Wavelet Extrema Representation

Abstract: The wavelet extrema representation originated by Stéphane Mallat is a unique framework for low-level and intermediate-level (feature) processing. In this paper, we present a new form of wavelet extrema representation generalizing Mallat's original work. The generalized wavelet extrema representation is a feature-based multiscale representation. For a particular choice of wavelet, our scheme can be interpreted as representing a signal or image by its edges, and peaks and valleys at multiple scales. Such a representation is shown to be stable—the original signal or image can be reconstructed with very good quality. It is further shown that a signal or image can be modeled as piecewise monotonic, with all turning points between monotonic segments given by the wavelet extrema. A new projection operator is introduced to enforce piecewise monotonicity of a signal in its reconstruction. This leads to an enhancement to previously developed algorithms in preventing artifacts in reconstructed signal.

Summary

1. What is the original contribution of this work?

The original contribution of our work is: (1) given a new form of signal representation using the local extrema of a wavelet transform, and given the representation a perceptual interpretation; (2) conceptualized modeling of a signal as piecewise monotonic, described an algorithm enforcing piecewise monotonicity, and used the concept and algorithm to improve the performance of signal reconstruction from the wavelet extrema.

2. Why should this contribution be considered important?

Edges, and peaks and valleys are important features in visual perception. Our scheme of signal representation in 2-D suggests essentially that these features, when observed at multiple scales, form a stable and accurate representation. We have a virtually reversible intermediate-level representation. This result is important to the understanding of the mechanism of image representation in biological vision, and the design of machine vision systems. The concept of modeling a signal or image as piecewise monotonic and the algorithm to enforce piecewise monotonicity are also important; their applications can go beyond the scope of wavelet extrema representation to solve problems such as image restoration and surface reconstruction.

3. What is the most closely related work by others and how does this work differ?

As suggested in the title, this work is a generalization to some previous one by others, particularly the work by Stéphane Mallat[17]. Overall, our work is complementary to the existing one, offering an alternative with new interpretations and improved performance. Nevertheless, the use of piecewise monotonicity as a constraint to reconstruction is completely new. We have provided a rigorous way to prevent artifacts resulting from spurious wavelet extrema in the reconstructed signal.

4. How can other researchers make use of the results of this work?

The wavelet extrema representation provides a framework for signal and image processing, and pattern analysis. Previous work based on this framework included image coding, denoising, contrast enhancement, stereo matching, edge and pattern classifications, and transient detection and removal. The continuing development of these applications and new ones will benefit from our improved framework of wavelet extrema representation. The perceptual interpretation we give to the wavelet extrema representation is also of interest to researchers who study biological vision.

This work has not been previously presented at or submitted to other conferences, workshops, or journals.

1 Introduction

The wavelet extrema representation originated by Stéphane Mallat is a new framework for image analysis and processing. It is an intermediate-level representation built on a wavelet transform of an image: only local extrema of the wavelet transform, or *wavelet extrema* for short, are kept to form a representation set. Depending on the wavelet used, the wavelet extrema often have some physical and perceptual meanings such as "edges" or "ridges" of the image.

Mallat and his colleagues have studied particularly the wavelet maxima representation[17], a special form of the wavelet extrema representation. Their work was motivated by Marr's conjecture that the edges at multiple scales may form a complete representation of an image[19]. By using a wavelet similar to the derivative of a Gaussian, Mallat and Zhong[17] showed that a signal or image can be represented effectively and efficiently by the wavelet maxima. They called it the *multiscale edge representation.* Meyer[20] showed that the multiscale edge representation is not complete in mathematical sense. However, signals and images reconstructed from their multiscale edges are often visually indistinguishable from the originals, making the multiscale edge representation, or more generally the wavelet extrema representation, a practical framework for signal and image analysis and processing.

It is notable that one can reconstruct the low-level sample representation of an image from its wavelet extrema without significant loss of information. This makes the wavelet extrema representation different from many other intermediate-level (feature) representations which cannot run reversely. Indeed, the traditional process of obtaining an intermediate-level representation is often a bottom-up abstraction; one cannot go back to the raw samples from the extracted features. A particular virtue of a reversible wavelet extrema representation is that in addition to the bottom-up feature extraction and analysis, one can *process* the original image by manipulating its wavelet extrema. As such, a wavelet extrema representation is a suitable framework for both low- and intermediate-level processing. Even better, such a framework makes it possible to combine low- and intermediate-level processing, with each benefiting from one another. Additionally, the use of wavelets enables one to extract, analyze, and manipulate these features at multiple scales with a computationally efficient wavelet transform. To date, the wavelet extrema representation has been successfully used in low- and intermediate-level signal and image processing. These applications include image coding[18, 10], denoising[16, 13, 11], contrast enhancement[12], edge classification[16, 23], shape description[21], and transient detection and removal[4].

In this paper, we present a new form of the wavelet extrema representation generalizing Mallat's original work. The generalized wavelet extrema representation is a feature-based multiscale representation. The "features" can have different physical and perceptual meanings depending on the choice of wavelet. We designed an algorithm for reconstructing a signal or image from the generalized wavelet extrema representation. The algorithm, based on the previous work developed by others, offers an improvement on the quality of reconstruction. In particular, our algorithm incorporates a new projection operator that provides a rigorous solution to the problems of inconsistency and artifacts caused by spurious wavelet extrema.

In the presentation to follow, we will first introduce in Section 2 the basic concepts of wavelet extrema, and the wavelet extrema representation developed by Mallat. Some related

work by others on the reconstruction problem is also reviewed. In Section 3, we present our generalized form of wavelet extrema representation. We give some intuitive ideas motivating and interpreting such representation, and introduce a new way for modeling and enforcing data consistency with the wavelet extrema. This leads to a refined reconstruction algorithm. Experimental results are presented in Section 4; we demonstrate the generalized wavelet representation with a test 1-D signal and a 2-D image. The quality of the reconstruction is evaluated. Finally, Section 5 concludes our presentation.

2 Wavelet Transform, Wavelet Extrema, and Associated Representations

In this section, we review the basics of wavelet transform, wavelet extrema and the associated representations. Because all the representations for 2-D images are generalized from those for 1-D signals, we will go through 1-D representations in sufficient detail. Our review is selective, however, with a purpose to provide a ground for the presentation in the following sections. References are provided for readers who are interested in a more comprehensive investigation of related work.

2.1 Finite-Scale Wavelet Transform Representation

Let $\psi(x) \in L^2(R)$ be an admissible dyadic wavelet and $\phi(x) \in L^2(R)$ be a scaling function associated with ψ[20]. The dilation of ψ and ϕ by $s = \{2^j\}_{j \in Z}$ is defined as

$$\psi_{2^j}(x) = \frac{1}{2^j}\psi(\frac{x}{2^j}),$$

and

$$\phi_{2^j}(x) = \frac{1}{2^j}\phi(\frac{x}{2^j}).$$

It is well-known that $\{\psi_{2^j}(x)\}_{j \in Z}$ have the characteristics of bandpass filters and $\{\phi_{2^j}(x)\}_{j \in Z}$ of lowpass filters. The approximations to a 1-D signal $f(x)$ by ψ_{2^j} and ϕ_{2^j} are given by

$$W_{2^j} f(x) = f * \psi_{2^j}(x), \tag{1}$$

and

$$S_{2^j} f(x) = f * \phi_{2^j}(x), \tag{2}$$

where "*" denotes convolution operation. In practice, the observation of any signal is limited between a nonzero small (fine) scale and a finitely large (coarse) scale. Without loss of generality, the smallest scale can be normalized to 1; the largest scale is 2^J where J is

determined by the size of the observation. A wavelet transform representation of $f(x)$ on the finite range of scales, $1 < s < 2^J$, is given by

$$\mathcal{W}f = \{(W_{2^j} f(x))_{1 \le j \le J}, S_{2^J} f(x)\}. \tag{3}$$

where $\mathcal{W}$ is a dyadic wavelet transform operator. Eq. (3) is interpreted as a multiresolution representation. The information lost in smoothing $S_{2^{j-1}} f(x)$ to $S_{2^j} f(x)$ is stored in $W_{2^j} f(x)$, called the "detail signal"[14]. The original signal $f(x)$ can be recovered by an inverse wavelet transform operation $\mathcal{W}^{-1}$[14]. The $\mathcal{W}^{-1}$ starts with $S_{2^J} f(x)$ at scale 2^J and adds details $W_{2^j} f(x)$ recursively at each, increasingly finer scale.

In two dimensions, oriented wavelets can be used to generate the wavelet transform representation[15]. We are particularly interested in constructing a representation using two perpendicularly oriented wavelets $\psi^1(x,y)$, $\psi^2(x,y)$, and the associated scaling function $\phi(x,y)$. To simplify the discussion, we express the two perpendicularly oriented wavelets in a vector form, $\vec{\psi}(x,y) = [\psi^1(x,y), \psi^2(x,y)]^t$. The dilation of the 2-D wavelet and scaling function are defined in a similar way to 1-D:

$$\vec{\psi}_{2^j}(x,y) = \begin{bmatrix} \psi^1_{2^j}(x,y) \\ \psi^2_{2^j}(x,y) \end{bmatrix} = \frac{1}{2^{2j}} \begin{bmatrix} \psi^1(\frac{x}{2^j}, \frac{y}{2^j}) \\ \psi^2(\frac{x}{2^j}, \frac{y}{2^j}) \end{bmatrix}$$

and

$$\phi_{2^j}(x,y) = \frac{1}{2^{2j}} \phi(\frac{x}{2^j}, \frac{y}{2^j}).$$

For an image $f(x,y) \in L^2(R^2)$, its bandpass approximations by the oriented wavelets, and lowpass approximation by the scaling function at scale 2^j are defined by

$$\overrightarrow{W_{2^j} f}(x,y) = \begin{bmatrix} W^1_{2^j} f(x,y) \\ W^2_{2^j} f(x,y) \end{bmatrix} = \begin{bmatrix} f * \psi^1_{2^j}(x,y) \\ f * \psi^2_{2^j}(x,y) \end{bmatrix} \tag{4}$$

and

$$S_{2^j} f(x,y) = f * \phi_{2^j}(x,y). \tag{5}$$

A wavelet transform representation of $f(x,y)$ on a finite range of scales, $1 < s < 2^J$, is given by

$$\mathcal{W}f = \{(\overrightarrow{W_{2^j} f}(x,y))_{1 \le j \le J}, S_{2^J} f(x,y)\}. \tag{6}$$

We refer readers to [7, 14, 15, 20] for an extensive coverage of wavelet theory and details of computing wavelet transforms.

2.2 Wavelet Extrema Representation

A wavelet extrema representation of a signal or image is built upon the wavelet transform. We first consider a 1-D signal in its wavelet transform representation (3). Let A_{2^j} be the set of the wavelet extrema at scale 2^j:

$$A_{2^j}[f(x)] = \{[x_i, W_{2^j} f(x_i)] : \mid W_{2^j} f(x) \text{ has local extrema at } x = x_i\}. \tag{7}$$

Then the collection

$$\{A_{2^j}[f(x)]_{1 \le j \le J}, S_{2^J} f(x)\} \tag{8}$$

is called a wavelet extrema representation of $f(x)$. Note that the representation set includes wavelet extrema at all scales plus the lowpass approximation of $f(x)$ at the coarsest scale, 2^J.

In two dimensions, we first define the length and angle of $\overrightarrow{W_{2^j} f}(x, y)$ by

$$\rho_{2^j} f\ (x, y) \stackrel{\text{def}}{=} |\overrightarrow{W_{2^j} f}\ (x, y)| = \sqrt{\left(\mathcal{W}^1_{2^j} f(x, y)\right)^2 + \left(\mathcal{W}^2_{2^j} f(x, y)\right)^2} \tag{9}$$

and

$$\theta_{2^j} f(x, y) \stackrel{\text{def}}{=} \arctan\left[\frac{\mathcal{W}^2_{2^j} f(x, y)}{\mathcal{W}^1_{2^j} f(x, y)}\right]. \tag{10}$$

The set of 2-D extrema at scale 2^j is

$$A_{2^j}[f(x, y)] \ = \ \left\{\left[(x_i, y_i); \overrightarrow{W_{2^j} f}(x_i, y_i)\right] : \left| \begin{array}{l} \rho_{2^j} f(x_i, y_i) \text{ has local extrema at} \\ (x_i, y_i) \text{ along the direction } \theta_{2^j} f(x_i, y_i) \end{array} \right.\right\} \tag{11}$$

Finally, the wavelet extrema representation of image $f(x, y)$ is given by

$$\{A_{2^j}[f(x, y)]_{1 \le j \le J}, S_{2^J} f(x, y)\}. \tag{12}$$

A special form of the wavelet extrema representation, called the *wavelet maxima representation*, has been studied extensively by Mallat and his colleagues[17, 16], and others[1, 20]. Many applications have also been developed based on the wavelet maxima representation [16, 10, 13, 12]. The representation set in a wavelet maxima representation is a subset of the wavelet extrema set defined by (7) or (11): only local maxima of $|W_{2^j} f(x)|$ or $|\overrightarrow{W_{2^j} f}(x, y)|$ are used. Mallat and Zhong designed a special family of wavelets such that

$$\psi(x) = \frac{d\phi}{dx}(x)$$

in 1-D and

$$\vec{\psi}(x,y) = \nabla(\phi(x)\phi(y)) = \frac{\partial\phi}{\partial x}(x)\phi(y) + \phi(x)\frac{\partial\phi}{\partial y}(y)$$

in 2-D. It can be shown that with these wavelets, the wavelet transform defined by (1) or (4) generates "multiscale gradients"[11]. Then, the wavelet maxima are the local maxima of the multiscale gradients along the gradient angle. The local maxima of gradients are the points of sharp variations in signal or image intensity; they are "edge points". Indeed, if $\phi(x)$ is a Gaussian, the process of obtaining the wavelet maxima is similar to applying the Canny edge detector[2] at dyadic scales. This is why the wavelet maxima representation is also called the "multiscale edge representation"[17].

Although the wavelet maxima are sufficient to characterize a signal, it adds no burden to adopt the superset—the wavelet extrema. There are additional advantages to work with the extrema instead of only the maxima. In the rest of the paper, we shall address mainly the wavelet extrema representation. Most algorithms associated with the wavelet extrema representation can be used with the wavelet maxima representation with a little modification.

2.3 Signal Reconstruction from Wavelet Extrema

A fundamental issue in the development of the wavelet extrema representation is the accurate and stable reconstruction of a signal from its wavelet extrema representation (8) or (12). This reconstruction process can be broken down into two steps: First, the wavelet transform representation of the signal is reconstructed from the wavelet extrema representation; then an inverse wavelet transform is computed. The key to the reconstruction is in the first step. Note that the lowpass part, $S_{2^J}f$, of the wavelet transform representation is retained in the wavelet extrema representation. Therefore, we need to reconstruct only the highpass part of the wavelet transform. In the 1-D case, this amounts to finding a sequence of functions $\{g_j(x)\}_{1\le j\le J}$. Then the reconstructed wavelet transform representation can be written as

$$\Omega \stackrel{\text{def}}{=} \{(g_j(x))_{1\le j\le J}, S_{2^J}f(x)\}.$$

Generally speaking, two constraints can be imposed on the reconstruction. The first of these states that since Ω is a wavelet transform representation, it must be in the range space of the wavelet transform for a particular choice of wavelet. The second constraint imposes that $\{g_j(x)\}_{1\le j\le J}$ in Ω has exactly the same extrema as $A_{2^j}[f(x)]_{1\le j\le J}$ in (8). For the ease of computation, the second constraint is often further decomposed into two sub-constraints such that one imposes that $\{g_j(x)\}_{1\le j\le J}$ pass all points in $A_{2^j}[f(x)]_{1\le j\le J}$ and the other requires these points to be the extrema, and the only extrema of $\{g_j(x)\}_{1\le j\le J}$. Mathematically, a constraint may be used to define a set consisting of all functions satisfying the constraint. Thus we have up to three sets:

V: the range space of the wavelet transform, containing all sequences of functions $\{v_j(x)\}_{1\le j\le J}$ such that $v_j(x)$ satisfies the reproducing kernel equation for the chosen wavelet[17];

Γ: the set of all sequences of functions $\{h_j(x)\}_{1\le j\le J}$ satisfying

$$\forall (x_i, W_{2^j} f(x_i)) \in A_{2^j}[f(x)]_{1\le j\le J},\ \ h_j(x_i) = W_{2^j} f(x_i); \tag{13}$$

Z: the set of all sequences of functions $\{z_j(x)\}_{1\le j\le J}$ such that

$$\forall x_i \in A_{2^j}[f(x)]_{1\le j\le J},\ \ z_j(x) \text{ has local extrema at and only at } x = x_i. \tag{14}$$

An admissible solution $\{g_j(x)\}_{1\le j\le J}$ to the reconstruction problem must lie in the intersection of V, Γ, and Z. A common way to compute the intersection of multiple sets is to project alternately onto these sets. The convergence of this alternating projection is guaranteed if all sets are convex and closed[24]. It can be shown that both V and Γ are closed convex sets; Z is convex if $A_{2^j}[f(x)]_{1\le j\le J}$ is the extrema set and nonconvex if it is the maxima set.

Denote by $\mathcal{P}_V$, $\mathcal{P}_\Gamma$, and $\mathcal{P}_Z$ the orthogonal projection operators to V, Γ, and Z, respectively. It has been shown[6] that for properly chosen synthesis wavelets, $\mathcal{P}_V$ can be conveniently built as a composition of the inverse and forward wavelet transform operators, i.e.,

$$\mathcal{P}_V = \mathcal{W} \circ \mathcal{W}^{-1}. \tag{15}$$

For a sequence of functions $\{g_j(x)\}_{1\le j\le J}$, the orthogonal projection to set Γ or Z amounts to finding in Γ or Z the nearest point to $\{g_j(x)\}_{1\le j\le J}$. Therefore, $\mathcal{P}_\Gamma$ and $\mathcal{P}_Z$ can be implemented as solving some minimization problems. More specifically, in implementing $\mathcal{P}_\Gamma$, we solve

$$\min\left(\sum_{j=1}^{J} \Theta_j(h_j(x) - g_j(x))\right) \ \text{ for } h_j(x) \in \Gamma. \tag{16}$$

where $\Theta_j(f)$ is a cost functional that must be defined. In [17], Mallat and Zhong defined a cost functional as

$$\Theta_j(f) = \int |f(x)|^2\, dx + 2^{2j} |\frac{d}{dx} f(x)|^2\, dx. \tag{17}$$

Then, $h_j(x)$ in (16) is obtained by solving piecewisely Euler equations with boundaries defined by the wavelet extrema[17, 25]. In [6], Cvetković and Vetterli used a least-squares cost functional

$$\Theta_j(f) = \Theta(f) = \int |f(x)|^2\, dx. \tag{18}$$

Computation of $h_j(x)$ is extremely simple with Θ_j defined by (18): one simply modifies $g_j(x)$ by replacing $g_j(x_i)$ with the value of the wavelet extrema in $A_{2^j}[f(x)]$.

The set Z has not been studied extensively and the implementation of $\mathcal{P}_Z$ is often *ad hoc*. This is probably because that Z is difficult to analyze and that applying $\mathcal{P}_V$ and $\mathcal{P}_\Gamma$

alone seems to produce very good reconstruction results. Carmona[3] showed the equivalence between alternating projections by $\mathcal{P}_V$ and $\mathcal{P}_\Gamma$ and the solution of an optimization problem, resulting in a noniterative reconstruction algorithm. The use of $\mathcal{P}_Z$ is for removing spurious extrema created in the process of projecting to V and Γ. For example, Mallat and Zhong used clipping to remove spurious extrema/maxima[17] in the reconstructed sequence $\{g_j(x)\}_{1\le j\le J}$ after each iteration of projections onto V and Γ. The clipping turns $\{g_j(x)\}_{1\le j\le J}$ into a new sequence belonging to Z. However, this new sequence is not necessarily the closest one to $\{g_j(x)\}_{1\le j\le J}$ in Z. Cvetković and Vetterli[6] used neighborhood averaging to remove spurious extrema. These authors did not consider the case that neighborhood averaging creates new, clustered extrema, therefore, their scheme cannot always transform $\{g_j(x)\}_{1\le j\le J}$ into a sequence in Z. We shall further study Z and $\mathcal{P}_Z$ in the next section.

In two dimensions, the three constraints and the asscoiated sets can be similarly defined. If we use the same notations as in 1-D, the $\mathcal{P}_V$ in 2-D has exactly the same form as in (15). The implementation of $\mathcal{P}_\Gamma$ in 2-D depends on the choice of the cost functional Θ_j. If (18) is chosen, we can use a straightforward generalization from 1-D implementation. If (17) is chosen, $\mathcal{P}_\Gamma$ can be implemented by minimizing (16) along x for $W^1_{2^j}f(x,y)$, and along y for $W^2_{2^j}f(x,y)$. Thus we have two separate 1-D minimization problems. The $\mathcal{P}_Z$ is often not considered in 2-D[17].

3 Generalized Wavelet Extrema Representation

We want to have a feature based representation where features are a sparse set of data extracted from the "raw data" and have some physical and perceptual meanings. The set of wavelet extrema at some scale 2^j, $A_{2^j}[f]$, is certainly a feature set. But the lowpass approximation of f at scale 2^J, $S_{2^J}f$, is not a feature set because it retains every sample. This side information is included in the wavelet extrema representations (8) and (12) because they are finite-scale representation. Indeed, if J can go infinitely large, $S_{2^J}f$ will vanish[14], and (8) and (12) will contain only the wavelet extrema. In this section, we will show that it is possible to replace $S_{2^J}f$ with some other features extracted from the wavelet transform and arrive at an all-feature representation on a finite range of scales, called a *generalized wavelet extrema representation* (GWER). Furthermore, we will provide a model for functions in set Z, and the associated projection operator $\mathcal{P}_Z$. Finally, a new reconstruction algorithm for GWER using $\mathcal{P}_V$, $\mathcal{P}_\Gamma$, and $\mathcal{P}_Z$ is presented.

3.1 Generalized Wavelet Extrema and GWER

We would like to extract some other features from the wavelet transform to replace the lowpass part $S_{2^J}f$ in the wavelet extrema representation. These features should be informative, revealing some important characteristics of the signal; they should be restraining, providing sufficient constraint as $S_{2^J}f$ does to the reconstruction; they should have reasonable requirement for data storage, preferably on the same order as that for $S_{2^J}f$. We are led to consider the local extrema of $S_{2^j}f$ for $1 \le j \le J$.

Let us recall that $S_{2^j}f$ is the lowpass approximation of f by ϕ_{2^j}, and $W_{2^j}f$ is the detail of the signal lost in smoothing from $S_{2^{j-1}}f$ to $S_{2^j}f$. Thus $S_{2^j}f$ and $W_{2^j}f$ are complementary to each other in representing and recovering $S_{2^{j-1}}f$. The local extrema of $S_{2^j}f$, like those of $W_{2^j}f$, are important features characterizing f. In the 1-D case, the local extrema of $S_{2^j}f$ are located between two consecutive extrema of opposite signs of $W_{2^j}f$. If we have $\psi(x) = \frac{d\phi}{dx}(x)$, the locations of local extrema in $S_{2^j}f$ are zero-crossing points in $W_{2^j}f$ between two consecutive local extrema of opposite signs. In the 2-D case, the local extrema of $S_{2^j}f$ are the locally lightest and darkest points in the image. These points are important in shading analysis and help characterize the shape of the image surface. Because the local extrema of $S_{2^j}f$ contain important information about f, they provide an additional constraint supplementary to that imposed by the local extrema of $W_{2^j}f$ for the reconstruction.

We illustrate the complementary nature of the local extrema of $S_{2^j}f$ and $W_{2^j}f$ by an image $f(x,y)$ in Figure 1. In this example we use the local maxima representation. Recall that the local maxima of $\overrightarrow{W_{2^j}f}(x,y)$ are defined by (11) as the local maxima of $|\overrightarrow{W_{2^j}f}(x,y)|$ along the direction of $\overrightarrow{W_{2^j}f}(x,y)$. In Figure 1, the local maxima of $\overrightarrow{W_{2^j}f}(x,y)$ and $S_{2^j}f(x,y)$ ($j = 1$ for illustration) correspond to, respectively, the boundary and the highlight points of a ball. Obviously, these points are all perceptually very important in recognizing the shape and dimension of the object. We are hoping to be able to reconstruct the light intensity distribution of the ball from the information of the local maxima. If we have only the boundary information from the local maxima of $\overrightarrow{W_{2^j}f}(x,y)$, the reconstruction has tremendous uncertainty because too little information is available about shading in the interior. The uncertainty will be reduced considerably if we specify the highlight point in the interior by the local maxima of $S_{2^j}f(x,y)$.

Let us define the set of local extrema of $S_{2^j}f(x)$ for a 1-D signal $f(x)$ as

$$B_{2^j}[f(x)] = \{[x_i, S_{2^j}f(x_i)] : \mid S_{2^j}f(x) \text{ has local extrema at } x = x_i\}. \tag{19}$$

The collection

$$\{A_{2^j}[f(x)], B_{2^j}[f(x)]\}_{1\le j\le J} \tag{20}$$

is called the *generalized wavelet extrema representation* (GWER) of $f(x)$.

The above definitions can be extended to 2-D in a straightforward way. We define $B_{2^j}[f(x,y)]$, the set of local extrema of $S_{2^j}f(x,y)$ and the 2-D GWER by

$$B_{2^j}[f(x,y)] = \{[(x_i,y_i), S_{2^j}f(x_i,y_i)] : \mid S_{2^j}f(x,y) \text{ has local extrema at } (x_i,y_i)\}. \tag{21}$$

and

$$\{A_{2^j}[f(x,y)], B_{2^j}[f(x,,y)]\}_{1\le j\le J} \tag{22}$$

We note that $S_{2^j}f$ is readily available from the computation of the discrete wavelet transform (DWT) using a recursive pyramid algorithm[17]. Therefore, compared to Mallat's

wavelet extrema representation, the only additional computation required for the GWER is to extract the local extrema in $S_{2^j}f$ when the latter becomes available during the computation of the DWT.

3.2 Piecewise Monotonicity as a Model and Constraint

We mentioned in §2.3 that the set Z has not been well characterized and the implementation of $\mathcal{P}_Z$ is inadequate. In this section, we provide a general model for a signal of which the local extrema are known. This model rigorously characterizes set Z and defines a projection operator $\mathcal{P}_Z$. Furthermore, there exists a highly efficient scheme for numerical implementation of $\mathcal{P}_Z$.

Let us now re-examize the set Z defined by (14) in §2.3. The key to the establishment of a new model for Z is to realize that any function $z_j(x)$ in Z can be segmented in a way such that on each segment $z_j(x)$ is monotonic. A point x_i joining two consecutive monotonic segments is called a *turing point* of $z_j(x)$. Obviously, a turning point is where $z_j(x)$ attains a local extremum. Therefore, $z_j(x)$ can be viewed as consisting of piecewise monotonic segments; the turning points are the extremal points of $z_j(x)$. We have arrived at a new definition for set Z:

Z: the set of all sequences of functions $\{z_j(x)\}_{1\le j\le J}$ such that $z_j(x)$ is piecewise monotonic with turning points located at $\{x_i\} \in A_{2^j}[f(x)]$.

It can be shown that Z is a convex set. The projection of an arbitrary sequence of functions $\{g_j(x)\}$ to Z is to find in Z a closest approximation to $\{g_j(x)\}$. The projection operator $\mathcal{P}_Z$ can be implemented as a constrained minimization solving

$$\min\left(\sum_{j=1}^{J}\Theta_j(z_j(x)-g_j(x))\right) \quad \text{for } h_j(x)\in Z, \tag{23}$$

where the cost functional $\Theta_j(f)$ can be defined by either (17) or (18). Note that this minimization problem can be divided into separate, independent minimization of Θ_j over each monotonic segment of $z_j(x)$. Therefore, for two consecutive extremal points x_i and x_{i+1}, we minimize Θ_j subject to the constraint that $z_j(x)$ is monotonic on interval $[x_i, x_{i+1}]$. We do the same type of minimization for every monotonic segment defined by the extremal points in $A_{2^j}[f(x)]$. The extremal values at x_i and x_{i+1} will determine if $z_j(x)$ is monotonically increasing or decreasing on a particular segment.

It turns out that the key to implementing $\mathcal{P}_Z$ is to compute minimum-error monotonic approximation to a function. This problem has been studied in depth by Powell[22], Cullinan and Powell[5], Demetriou[8], and Demetriou and Powell[9]. These authors developed efficient algorithms for computing best discrete monotonic approximation under ℓ^1, ℓ^2, and ℓ^∞ norms. The ℓ^2-algorithm is particularly interesting to us. It can be directly used for numerical implementation of $\mathcal{P}_Z$ with the cost functional defined by (17) or (18). The algorithm has $o(n)$ time complexity, where n is the number of points in a monotonic segment.

Demetriou and Powell's algorithm can also be used in signal reconstruction from the wavelet maxima representation. In the case that two consecutive wavelet maxima at x_i and x_{i+1} have the same sign, there exist two monotonic segments that are divided by a non-zero local minimum in $[x_i, x_{i+1}]$. Demetriou and Powell's algorithm can be used to obtain a piecewise monotonic approximation. The location of the local minimum in $[x_i, x_{i+1}]$ is an independent variable in the least-squares minimization and will be optimally determined. We refer readers to [9] for the implementation details of Demetriou and Powell's algorithm.

In two dimensions, the generalization of our method would imply modeling an image $f(x, y)$ as consisting of piecewise monotonic surfaces. Unfortunately, the wavelet extrema do not segment $|\overrightarrow{W_{2^j} f}(x, y)|$ into piecewise monotonic surfaces. We take a suboptimal approach by applying the 1-D $\mathcal{P}_z$ independently to $W^1_{2^j} f(x, y)$ along x and $W^2_{2^j} f(x, y)$ along y.

3.3 Outline of Reconstruction Algorithm

The reconstruction algorithm for recovering a signal from the GWER defined by (20) is a modification of the schemes described in §2.3. The set Γ now contains all sequences of functions defined by the generalized wavelet extrema, including the local extrema of both $(W_{2^j} f(x))_{1 \le j \le J}$ and $(S_{2^j} f(x))_{1 \le j \le J}$. The projection to set Z by $\mathcal{P}_z$ described in §3.2 is also incorporated in the reconstruction process. We summarize the steps of our reconstruction algorithm for obtaining an estimate $\hat{f}(x)$.

Reconstruction Algorithm

1 Set initial values of $(\widehat{W_{2^j} f}(x))_{1 \le j \le J}$ and $(\widehat{S_{2^j} f}(x))_{1 \le j \le J}$ to zero for all x.

2 For j from J decrementing to 1, do recursively:

  2.1 Apply $\mathcal{P}_\Gamma$: Update $\widehat{W_{2^j} f}(x)$ and $\widehat{S_{2^j} f}(x)$ by computing (16)

  2.2 Apply $\mathcal{P}_z$: Update $\widehat{W_{2^j} f}(x)$ and $\widehat{S_{2^j} f}(x)$ by computing (23)

  2.3 Update $\widehat{S_{2^{j-1}} f}(x)$ by computing a one-step inverse wavelet transform from $\widehat{W_{2^j} f}(x)$ and $\widehat{S_{2^j} f}(x)$.

  At the end of Step 2, we obtain an estimate $\widehat{S_1 f}(x) = \hat{f}(x)$.

3 Apply wavelet transform ($\mathcal{W}$) to $\hat{f}(x)$ to obtain an new estimate of $(\widehat{W_{2^j} f}(x))_{1 \le j \le J}$ and $(\widehat{S_{2^j} f}(x))_{1 \le j \le J}$.

4 Repeat Steps 2 and 3 for a number of iterations. The final estimate of $\hat{f}(x)$ is given at the end of Step 2 of the last iteration.

The above algorithm can be directly used in two dimensions with slight modifications in Steps 2.1 and 2.2. In Step 2.1, we must use the cost functional Θ_j defined by (18). In Step 2.2, we compute (23) for rows of $W^1_{2^j} f(x, y)$, columns of $W^2_{2^j} f(x, y)$, and both rows and columns of $S_{2^j} f(x, y)$.

4 Experiments

We have tested GWER with a large number of 1-D signals and 2-D images. We present two cases here. In both cases, we used a cubic spline wavelet. This wavelet is among a family of wavelet multiscale edge detectors designed by Mallat and Zhong[17]. Therefore, the generalized wavelet extrema can be interpreted as edges, and peaks and valleys at multiple scales.

Figure 2 shows a 1-D test signal and a reconstruction of the signal from its GWER. The signal consists of different edge profiles (step, ramp, and exponential) embedded in Gaussian white noise. The number of samples is 256, therefore, the largest scale $J = \log_2(256) = 8$. The GWER of the signal is shown in Figure 3. The reconstructed signal shown was obtained with 50 iterations, reaching a SNR of 33.9 dB. The dependency of the reconstruction performance on the number of iterations is shown in Figure 4. In general, 20 iterations seem to be sufficient for most applications. In Figure 4, we also compared the performance of reconstructions with and without using $\mathcal{P}_z$. We found the quality of reconstruction using $\mathcal{P}_z$ is consistently better, by a margin of about 1.5 dB over that without using $\mathcal{P}_z$. This confirms the effectiveness of $\mathcal{P}_z$.

Figure 5 is a 2-D case. The original image is a $128 \times 128 \times 8$ Lenna. Its GWER is shown for $J = 7$ dyadic scales. Note that $\overrightarrow{W_{2^j} f}$ is vector-valued, so are its local extrema. In Figure 5, the magnitude of the local extrema of $\{\overrightarrow{W_{2^j} f}\}_{1 \le j \le 7}$ is shown on the first column, the angle on the second column. The local extrema of $\{S_{2^j} f\}_{1 \le j \le 7}$ are shown on the third column. A reconstructed image, obtained with 20 iterations and shown on the upper right, has a SNR of 29.0 dB.

Our results from other test signals and images are consistent with the results shown here. These results suggests that the GWER is a stable representation; signals and images can be reconstructed from their GWER with sufficient quality for practical applications. In fact, the reconstructed signals and images are visually indistinguishable from the originals. We also observed that the number of wavelet extrema decreases rapidly as scale becomes coarse. This suggests that a GWER using fewer scales ($J < \log_2(N)$) may suffice in many applications.

5 Conclusion

We have presented a new form of wavelet extrema representation for 1-D signals and 2-D images. We illustrate that the local extrema of $S_{2^j} f$ in a wavelet transform are important features and can be used to replace $S_{2^J} f$ in the previously developed schemes of wavelet extrema representation. This leads to a generalized multiscale feature representation. For a particular choice of wavelet, the GWER in 2-D has an interpretation of representing an image by its edges, and peaks and valleys at multiple scales. Our experimental results suggest that the GWER is a stable representation. The quality of signals and images reconstructed from their GWER is sufficiently good for practical applications; we have a virtually reversible intermediate-level (feature) representation. We also developed a new projection operator that has further enhanced the reconstruction quality.

This work was performed under the auspices of the U.S. Dept. of Energy at LLNL under Contract No. W-7405-Eng-48.

References

[1] Z. Berman and J.S. Baras, "Properties of the multiscale maxima and zero-crossings representations," *IEEE Trans. Signal Proc.*, Vol. 41, pp. 3216-3231, Dec. 1993.

[2] J. Canny, "A computational approach to edge detection," *IEEE Trans. Pattern Anal. and Machine Intell.*, Vol. PAMI-8, pp. 679-698, Nov. 1986.

[3] R.A. Carmona, "Variations on the reconstruction algorithm of Mallat and Zhong," preprint, Dept. of Mathematics, UC Irvine, 1993.

[4] R.A. Carmona, "Wavelet identification of transients in noisy time series," in *Mathematical Imaging: Wavelet Applications in Signal and Image Processing*, Proc. of SPIE, vol. 2034, 1993.

[5] M.P. Cullinan and M.J.D. Powell, "Data smoothing by divided differences," in *Numerical Analysis*, A. Dold and B. Eckmann, Eds., Springer-Verlag, 1982.

[6] Z. Cvetković and M. Vetterli, "Discrete-time wavelet extrema representation: design and consistent reconstruction," *IEEE Trans. on Signal Processing*, vol. 43, No. 3, pp. 681-93, Mar. 1995.

[7] I. Daubechies, "Orthonormal bases of compactly supported wavelets II, Variations on a theme," *SIAM J. Math. Anal.*, Vol. 24, pp. 499-519, Mar. 1993.

[8] I.C. Demetriou, "A characterization theorem for the discrete best monotonic approximation problem," *Mathematics of Computation*, Vol. 35, pp. 191-195, 1990.

[9] I.C. Demetriou and M.J.D. Powell, "Least squares smoothing of univariate data to achieve piecewise monotonicity," *IMA Journal of Numerical Analysis*, Vol. 11, pp. 411-432, 1991.

[10] J. Froment and S. Mallat, "Second generation compact image coding with wavelets," in *Wavelet: A Tutorial in Theory and Applications,* C.K. Chui, Ed., Academic Press, San Diego, 1992, pp. 655-678.

[11] J. Lu, "Signal recovery and noise reduction with wavelets," Ph.D. Dissertation, Dartmouth College, Hanover, NH, 1993.

[12] J. Lu, D.M. Healy, Jr. and J.B. Weaver, "Contrast enhancement of medical images using multiscale edge representation," *Optical Engineering*, Vol. 33, No. 7, pp. 2151-2161, July 1994.

[13] J. Lu, J.B. Weaver and D.M. Healy Jr, "Noise reduction with multiscale edge representation and perceptual criteria," in *Proc. IEEE-SP Intl. Symp. on Time-Frequency and Time-Scale Analysis*, 1992.

[14] S.G. Mallat, "A theory of multiresolution signal decomposition: the wavelet representation," *IEEE Trans. Pattern Anal. and Machine Intell.*, vol. PAMI-11, pp. 674-693, July 1989.

[15] S.G. Mallat, "Multifrequency channel decomposition of images and wavelet models," *IEEE Trans. Acoust. Speech and Signal Proc.*, Vol. 37, pp. 2091-2110, Dec. 1989.

[16] S. Mallat and W.-L. Hwang, "Singularity detection and processing with wavelets," *IEEE Trans. Info. Theory*, Vol. 38, No. 2, pp. 617-643, March 1992.

[17] S.G. Mallat and S. Zhong, "Characterization of signals from multiscale edges," *IEEE Trans. Pattern Anal. and Machine Intell.*, Vol. 14, pp. 710-732, July 1992.

[18] S. Mallat and S. Zhong, "Compact image coding from edges with wavelet," in *Proc. of ICASSP'91.*

[19] D. Marr, *Vision*, W.H. Freeman, San Francisco, CA, 1982.

[20] Y. Meyer, *Wavelets: Algorithms and Applications*, Philadelphia: SIAM, 1993.

[21] Y. Nakamura and T. Yoshida, "Learning two-dimensional shapes using wavelet local extrema," *Proceedings of the 12th IAPR International Conference on Pattern Recognition*, Jerusalem, Israel, Oct. 1994.

[22] M.J.D. Powell, *Approximation Theory and Methods*, Cambridge,UK: Cambridge University Press, 1981.

[23] J.B. Weaver, D.M. Healy,Jr., H. Nagy, S.P. Poplack, J. Lu, T. Sauerland and D. Langdon, "Classification of masses in digitized mammograms with features in the wavelet transform domain," in *Wavelet Applications*, H.H. Szu, Editor, Proc. SPIE, Vol. 2242, pp. 704-710, 1994.

[24] D. Youla and H. Webb, "Image restoration by the method of convex projections," *IEEE Trans. Med. Imaging*, Vol. 1, pp. 81-101, Oct. 1982.

[25] S. Zhong, "Edge representation from wavelet transform maxima," Ph.D. Dissertation, New York University, 1990.

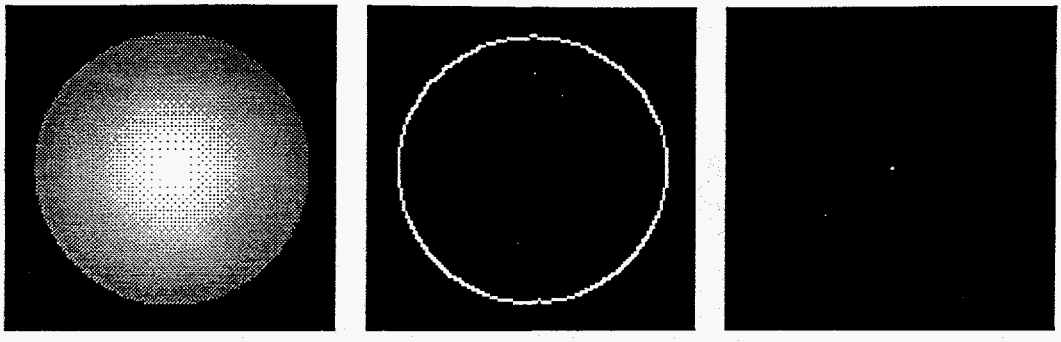

(a) (b) (c)

Figure 1: A synthetic image and its wavelet maxima at scale 2^1. (a) An image of a ball; (b) the local maxima of $\overrightarrow{W_{2^1}f}$, which are the edges of the ball; only the magnitude of the local maxima is shown; (c) the local maxima of $S_{2^1}f$, which are the highlight points of the ball. Obviously, the local maxima of $\overrightarrow{W_{2^j}f}$ and $S_{2^j}f$ are both important features in perception. The combination of them is a special form of our generalized wavelet extrema representation.

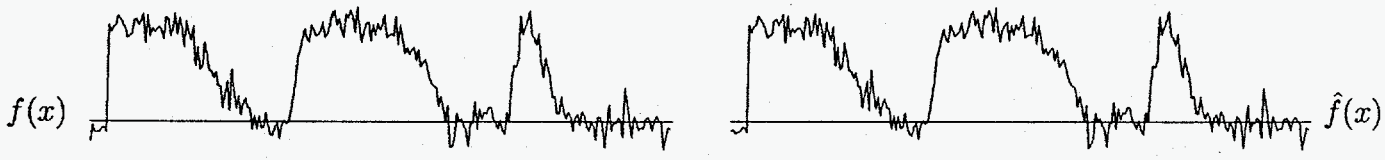

(a) (b)

Figure 2: Reconstruction of a 1-D signal from its GWER. (a) the original signal (256 samples); (b) a reconstruction from the GWER with 50 iterations; $SNR = 33.9dB$. The GWER of the signal is shown in Figure 3.

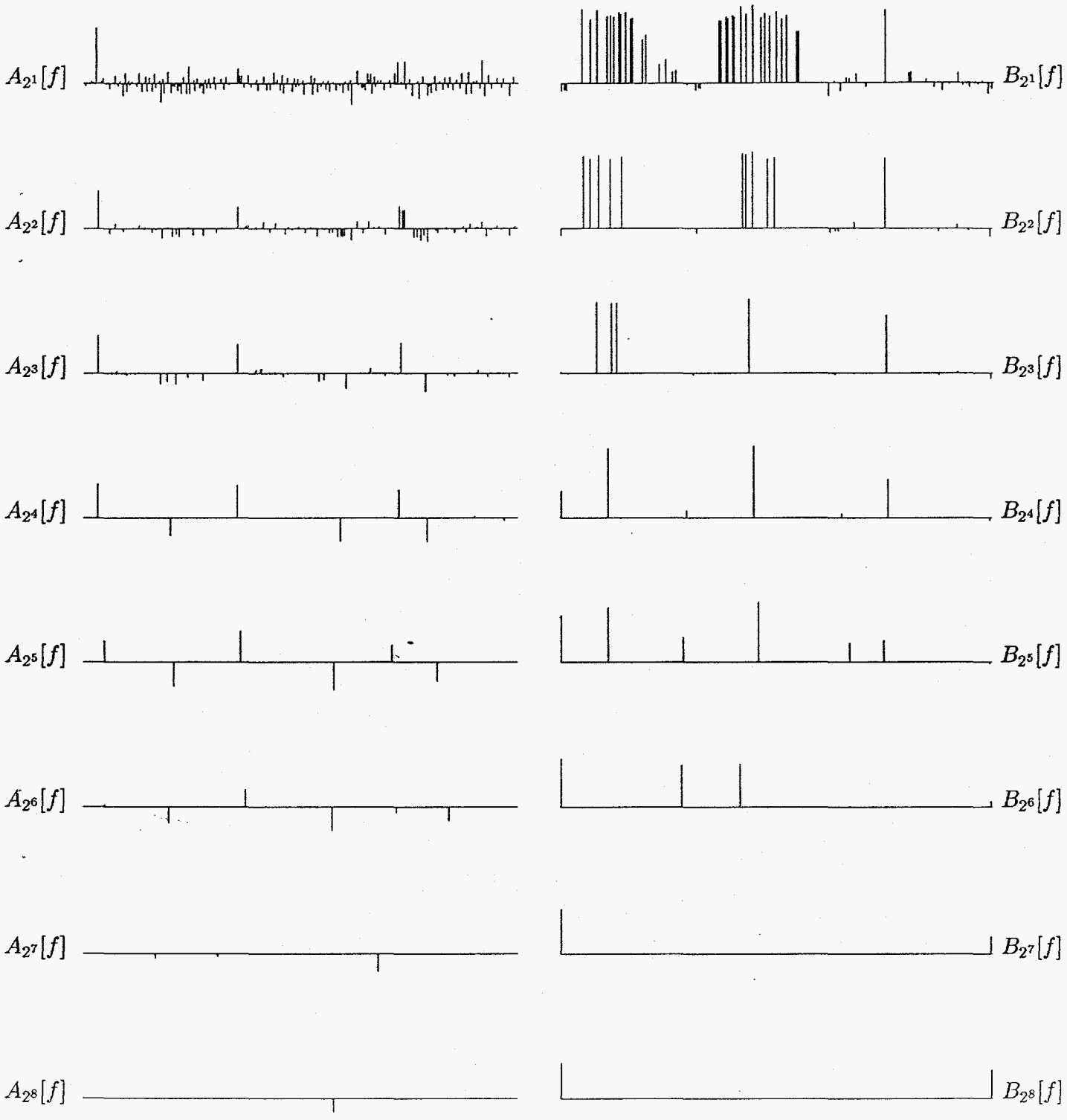

Figure 3: The GWER of the signal in Figure 2(a). The local extrema of $(W_{2^j} f)_{1 \leq j \leq 8}$ and $(S_{2^j} f)_{1 \leq j \leq 8}$ are shown on left and right columns, respectively.

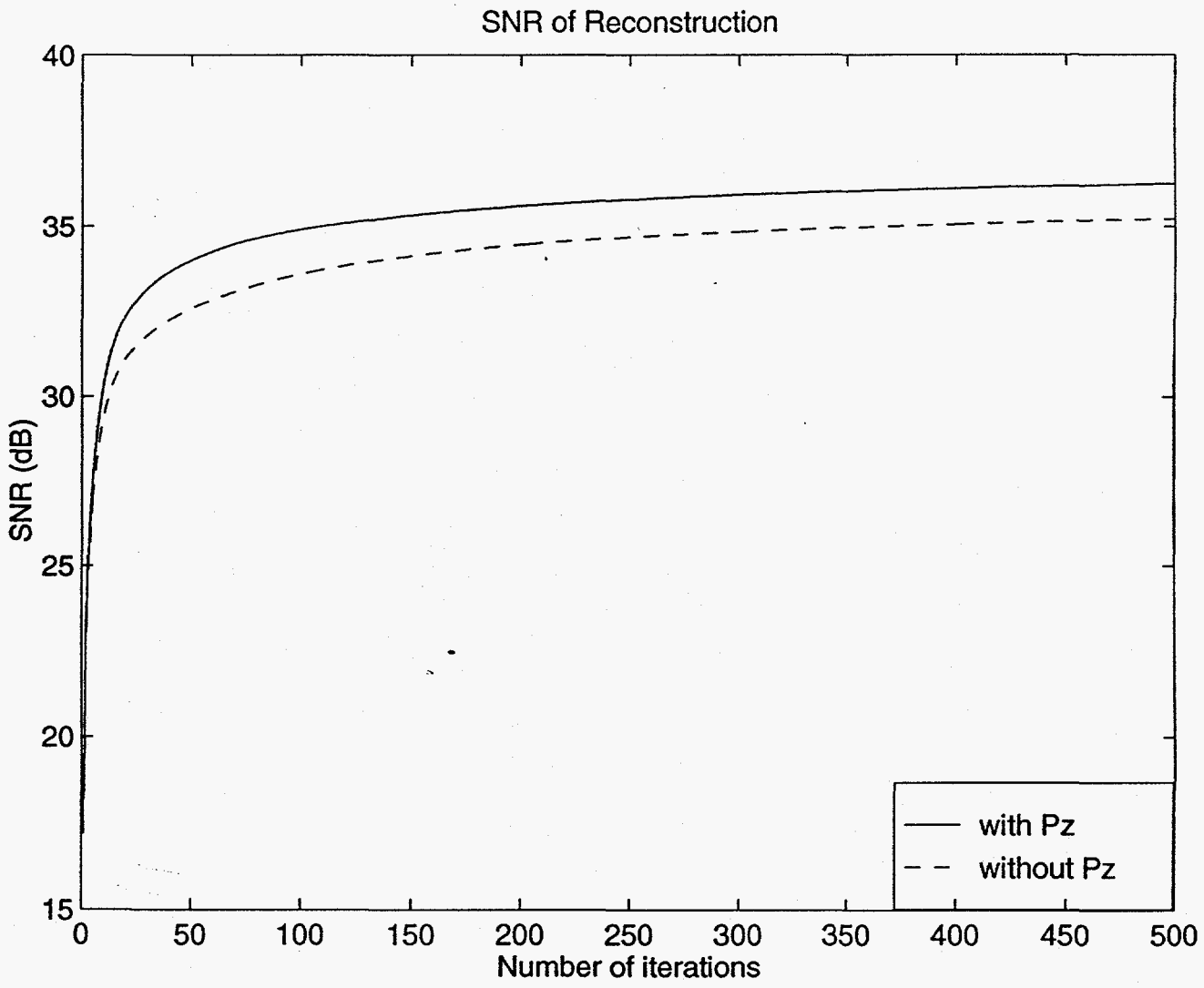

Figure 4: Reconstruction performance vs. number of iterations in the reconstruction of the signal in Figure 2. A comparison is made between reconstructions with and without using $\mathcal{P}_z$.

Original

Reconstructed

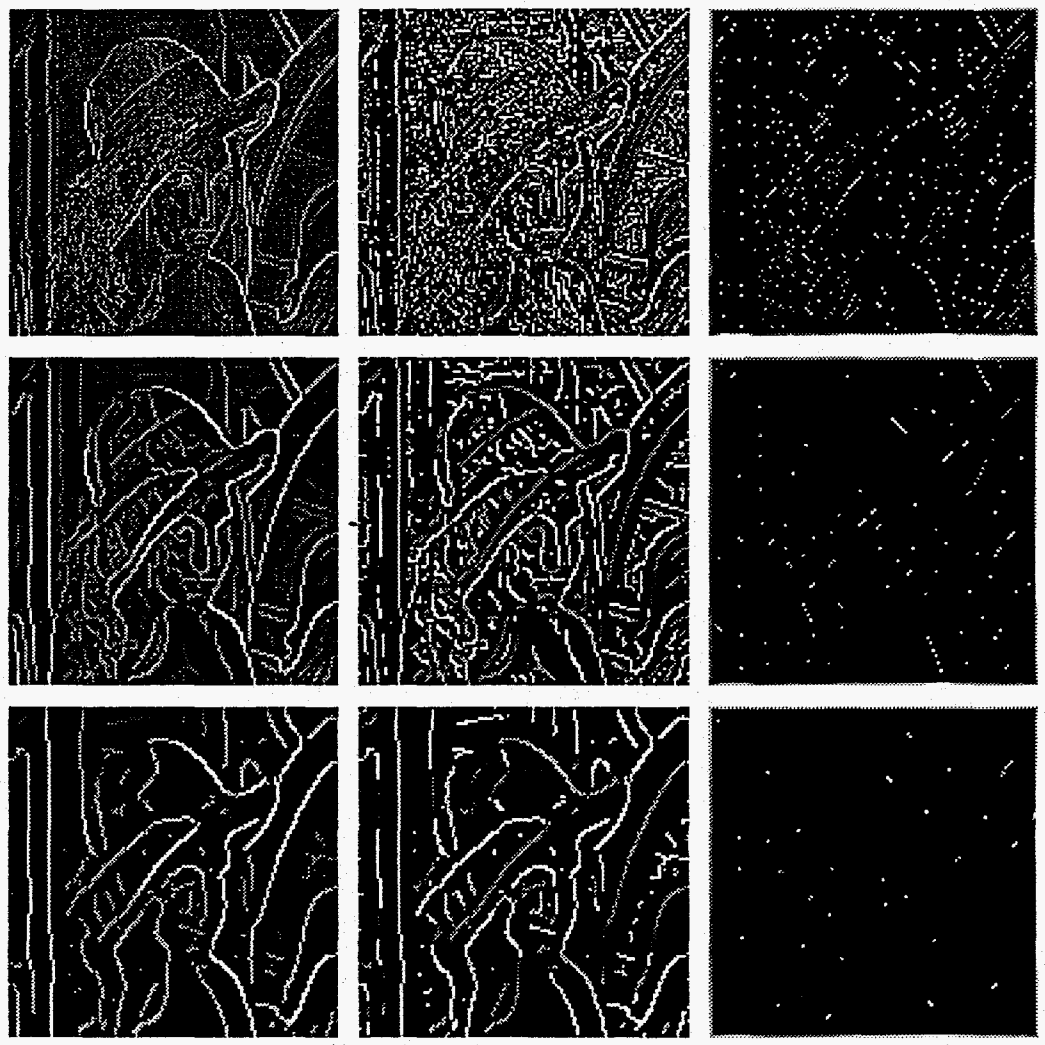

(Continued on next page)

Figure 5: Representation and reconstruction of an image from its generalized wavelet extrema. The first image on the top row is the original, Lenna, $128 \times 128 \times 8$; the second is a reconstruction from the GWER which is shown by rows 2–8. The first column of the GWER shows the magnitude images of the local extrema of $\{\overrightarrow{W_{2^j} f}\}_{1 \le j \le 7}$; the second column shows the angle images; the third column shows the local extrema of $\{S_{2^j} f\}_{1 \le j \le 7}$. The reconstructed image, obtained with 20 iterations, has a SNR of 29.0 dB.

Continued from previous page:

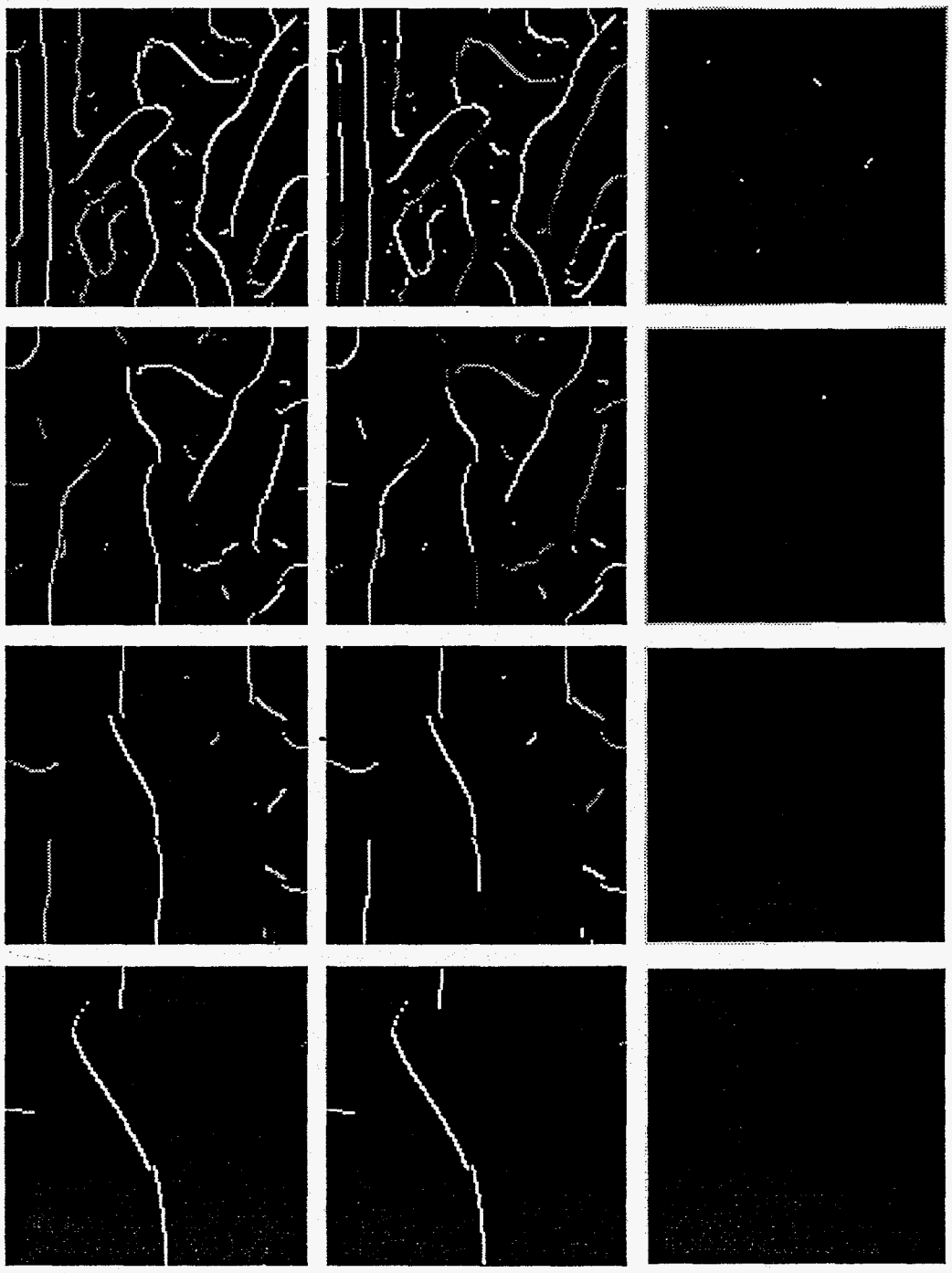

(Captions on previous page)